Chapter 2
Immobilization Methods for Observing Living Mammalian Suspended Cells by AFM

Imaging cellular topography is the basic application of AFM in cell biology. The studies about AFM cell imaging began in the early 1990s [1]. According to the different imaging environments, AFM cell imaging can be divided into two types, including imaging cells in air and imaging cells in liquid. For imaging cells in air, cells are chemically fixed to maximally maintain the native structures of the cells. The most commonly used chemical fixatives are 2.5% glutaraldehyde and 4% paraformaldehyde [2]. In 2005, Yang et al. [3] used AFM to image the interactions between nanoparticles and cells in air based on glutaraldehyde fixation and AFM images clearly showed the endocytosis of nanoparticles taking place during the process of internalization. In 2009, Wu et al. [4] investigated the membrane surface nanostructures of T lymphocytes by AFM imaging in air based on glutaraldehyde fixation, revealing that there were significant differences in the nanoscale cellular topography between resting T lymphocytes and activated T lymphocytes. The process of imaging chemically fixed cells in air is simple and the recorded AFM images are often with high spatial resolution, which is useful for visualizing the detailed structures of cell surface. However, the drying process can inevitably cause the changes of cellular structures, which produces difficulty in the interpretation of the obtained AFM images. Besides, in many cases, researchers are more interested in living cells, since the results from living cells can better reflect the real situations and allow investigating the real-time dynamics of cellular fine structures during physiological activities.

2.1 Current Status of Immobilizing Living Cell for AFM Imaging

The prerequisite of imaging living cells by AFM is immobilizing living cells firmly on a substrate to resist the lateral forces exerted by the scanning tip [5]. For the different cell types, the immobilization methods are varied. Adherent cells (e.g.,

M. Li, *Investigations of Cellular and Molecular Biophysical Properties by Atomic Force Microscopy Nanorobotics*, Springer Theses,
https://doi.org/10.1007/978-981-10-6829-4_2

fibroblasts, epithelial cells, and neurons) can directly grow on the substrate (e.g., petri dish, glass slide), and thus they can be imaged by AFM after being cultured for 1 or 2 days on the substrate [6]. Sometimes the substrate is coated by a layer of poly-L-lysine to promote cell adhesion [7]. For microbial cells (e.g., bacterium, yeast), they cannot naturally adhere to the substrate. Electrostatic adsorption method and porous polymer membrane method are commonly used to immobilize microbial cells [8]. In electrostatic adsorption, positively charged macromolecules such as poly-L-lysine are coated on the substrate so that the negatively charged microbial cells readily adsorb. Alternatively, cell suspensions are filtered through a porous polymer membrane by an injector, which can trap microbial cells in the pores of the polymer membrane. The polymer membrane is then attached to a substrate with double-sided adhesion tape. It should be noted that the porous polymer membrane immobilization method is based on commercial membranes and is thus best suited for round-shaped microbial cells whose sizes are comparable to the pore size. It is not well suited for rod-shaped cells [9]. In 2010, Fantner et al. [10] used high-speed AFM to image the morphological dynamics of *Escherichia coli* cells based on the poly-L-lysine method, clearly revealing the rougher of the cell surface after the stimulation of antimicrobial peptide. In 2010, Andre et al. [11] used the porous polymer membrane to immobilize the living *Lactococcus lactis* cells and observed the nanoscale organization of the peptidoglycan in the cell by AFM imaging.

The electrostatic adsorption and porous polymer membrane methods are not applicable for mammalian suspended cells (e.g., blood cells) which are much larger than microbial cells and have soft surface (microbial cells have stiff cell walls). There are no commercially available polymer membranes whose pores are comparable to the size of mammalian suspended cells. Researchers have used microwells fabricated in the silicon substrate to trap mammalian suspended cells (e.g., leukamia cells [12], chondrocytes [13]) for measuring cell mechanics. Although the microwells can help cells to withstand the lateral forces exerted by scanning tip, in the vertical direction there are no forces to attach the cells to the bottom of the well, causing that cells in the wells can easily be moved when being probed by AFM tip. Currently, the spatial resolution for AFM imaging of mamalian cells is only about 50 nm [14]; this is because the cell membranes are soft and dynamic in nature, which in turn causes the scanning tip to deform the cell membrane. Besides, there are adhesive interactions between the AFM tip and cell membrane [15]. All of these factors seriously influence the resolution of AFM imaging of mammalian cells and so far it has not been able to resolve single proteins on living cells.

2.2 Biological Experiment Platform Based on AFM Nanorobot

The biological experiment platform based on AFM nanorobot developed here includes AFM (Bruker, Santa Barbara, USA), cell incubator (Thermo Fisher, Waltham, USA), biological safety cabinet (Thermo Fisher, Waltham, USA), optical

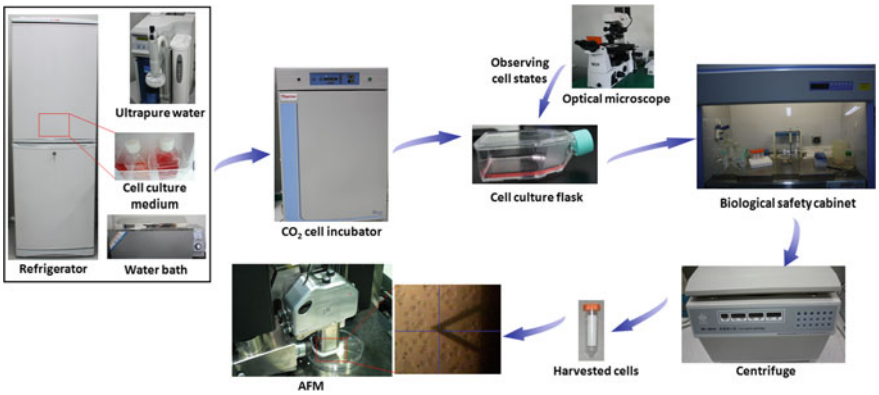

Fig. 2.1 AFM nanorobot biological experiment platform. Cells cultured in the CO_2 incubator are transported to the biological safety cabinet for sample preparation, and the samples are then transported to AFM for experiments, such as imaging cellular topography, measuring cellular mechanics, and recognizing molecular interactions on cell surface

microscope (Nikon, Tokyo, Japan), centrifuge (Zonkia, Hefei, China), refrigerator (Zhongke Meiling, Hefei, China), ultrapure water system (Millipore, Billerica, USA), and water bath, as shown in Fig. 2.1. Cell incubator provides the environment (37 °C, 5% CO_2) for cellular survival and proliferation in vitro. Cell culture mediums provide necessary nutrients that promote cell growth. Ultrapure water provides sterile deionized water for cell assay. The cell culture medium is stored in the refrigerator at 4 °C. The cell culture medium is heated to 37 °C in the water bath before being used. Optical microscope is used to observe the growth state of cells to judge whether or not cell passage is needed. The biological safety cabinet is used for related manipulations in the experiments, such as preparing cell culture medium, drug stimulation, and fluorescence staining. Centrifuge is used to harvest cells, which are then delivered to the workspace of AFM for various experiments.

With the established biological experiment platform, three types of adherent cells (MCF-7 human breast cancer cell line, HeLa human cervical cancer cell line, U251 human glioblastoma cell line) were imaged, as shown in Fig. 2.2. Under the guidance of optical microscope (Fig. 2.2a–c), the AFM probe was moved to the living cells to perform contact mode imaging. The three types of cells (MCF-7, HeLa, U251) firmly adhere to the substrate, which allows them easily imaged by AFM. Figure 2.2d, g are the AFM height image and corresponding deflection image of MCF-7 cells respectively. The scan size was 100 μm. We can see that four MCF-7 cells clustered together. MCF-7 cells were triangular or polygonal, and cellular edges were obviously discernible. Figure 2.2e, h are the AFM height image and corresponding deflection image of HeLa cells respectively. The scan size was 80 μm. Nine HeLa cells which adhered to the substrate were visible. Figure 2.2f, i are the AFM height image and corresponding deflection image of U251 cells respectively. The scan size was 120 μm. Comparing the three types of cells, we can

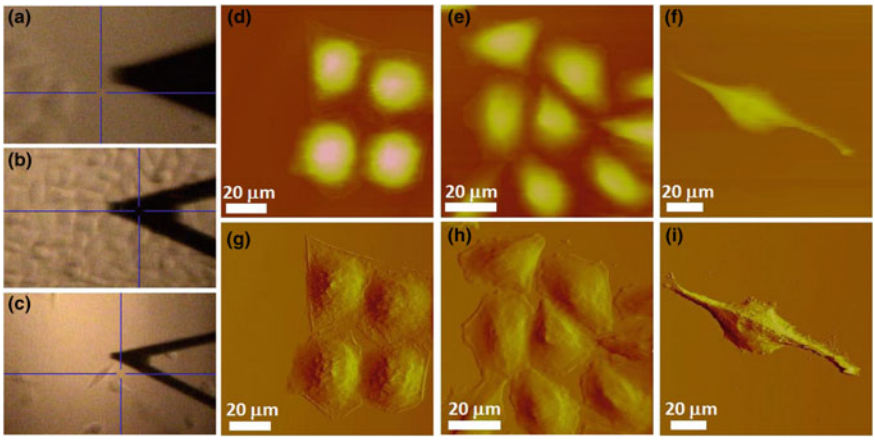

Fig. 2.2 AFM contact mode images of living adherent cells. (**a**–**c**) Under the guidance of optical image, the AFM tip was moved to the cells. (**d**–**f**) AFM height images of MCF-7 cells **d**, HeLa cells **e**, and U251 cells **f**. (**g**–**i**) Corresponding AFM deflection images of MCF-7 cells **g**, HeLa cells **h**, and U251 cells **i**

see that MCF-7 and HeLa cells had polygonal shape, while U251 cells were fusiform. This morphology structure caused that the diameter of U251 cells along the long axis was significantly larger than the size of MCF-7 and HeLa cells. Collectively, adherent cells can naturally grow and spread on the substrate, and thus facilitates AFM imaging on them.

2.3 Immobilizing Mammalian Suspended Cells by Micropillar Array

In order to image mammalian suspended cells, here an immobilization method combining micropillar mechanical trapping in the horizontal direction and poly-L-lysine electrostatic adsorption in the vertical direction was developed. Based on the method, AFM images of fine structures of lymphoma living cells were successfully recorded at tapping mode, and the schematic diagram is shown in Fig. 2.3. Current immobilization methods only consider trapping cells in the horizontal direction [12, 13]. Cells are still motile in the vertical direction, which makes it difficult to image the cell topography with AFM. Here micropillar array chip was fabricated on the silicon substrate which was then covered by a layer of poly-L-lysine, allowing cells trapped in both horizontal and vertical directions. Since cell surface was soft, tapping mode which can efficiently eliminate the influence of lateral forces exerted by the scanning tip on imaging was adopted.

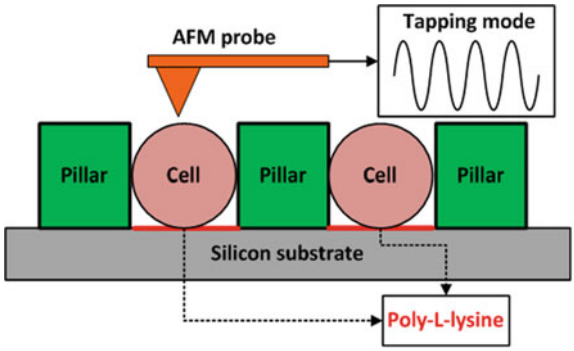

Fig. 2.3 Immobilizing mammalian suspended cells by micropillar trapping and poly-L-lysine electrostatic adsorption. Cellular morphology was acquired by AFM tapping mode imaging

The micropillar array chips were fabricated by photolithography technology [16]. The fabrication process includes photoresist application, exposure, etching, and stripping, as shown in Fig. 2.4a. Figure 2.4b is the photograph of a chip. The length, width, and height of a chip was 20, 10, and 1 mm respectively. The pillar height was 5 μm, and the pillar diameter was 10 μm. Because of the variable cell sizes, the distance between two adjacent pillars was designed with three sizes (5, 10, 15 μm). The chips were imaged by SEM and AFM. From the SEM images (Fig. 2.4c, d), we can see the ordered pillars. Figure 2.4e–g are the AFM height image, three-dimensional image, and section profile of the pillars respectively, showing that the actual height of the pillar was about 4 μm.

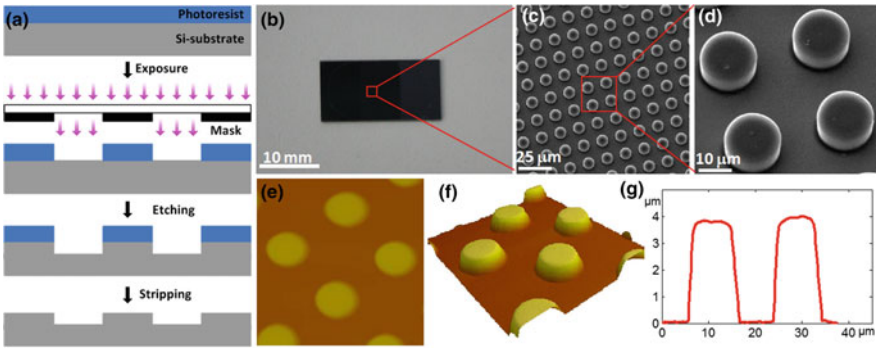

Fig. 2.4 Fabricating micro-pillar array chips with photolithography. **a** Fabricating principle. **b** Photograph of micro-pillar array chip. **c** SEM image of micro-pillar array. **d** SEM image of one unit of micro-pillar. (**e**, **f**) AFM images of micro-pillar unit. **e** Height image. **f** Three-dimensional image. **g** A section profile of two pillars

2.4 Imaging Living Mammalian Suspended Cells Based on Micro-Pillar Immobilization

In order to examine the effectiveness of the presented method, lymphoma Raji cells (a type of mammalian suspended cell) were used for tests. The experimental procedure was following. (1) Raji cells were cultured in RPMI-1640 medium containing 10% fetal bovine serum at 37 °C (5% CO_2) for 24 h. (2) Dilute 0.1% poly-L-lysine 10 times with Milli-Q ultrapure water (18.2 MΩ cm) and then drop the poly-L-lysine solution onto the pillar chips and stored at room temperature for air drying. (3) Add 5 ml of cell suspension into an eppendorf tube and centrifuge for 5 min at the speed of 1000 r/min. (4) After the centrifugation, the supernatant of the eppendorf tube was removed and then 1 ml fresh PBS was added into the tube. After stirring the solution with a pipette, a drop of solution was placed onto the poly-L-lysine-coated pillar array chip and incubated for 1 min. (5) The chip was attached to a glass slide using a small piece of double-sided adhesive tape and then placed into a Petri dish containing PBS. (6) After placing the Petri dish on the sample stage of AFM, AFM imaging was immediately performed. Under the guidance of optical microscope, AFM probe was moved to the cells trapped by pillars. The Si_3N_4 probe with a nominal spring constant of 0.12 N/m was used. Imaging was performed in tapping mode with a driving frequency of ~9 kHz. The scan rate was 0.5 Hz. The scan line was 256 and the sampling point for each scan line was also 256.

Figure 2.5 shows the results of imaging living Raji cells by AFM tapping mode based on the presented cell immobilization method. Figure 2.5a is the schematic diagram of trapping cells by pillars. Figure 2.5f is the optical image. Large-size scan was performed first to acquire the topography of the whole cell, and then small-size scan was performed to acquire the topography of the cellular local area. Figure 2.5b–e was the AFM height image, phase image, amplitude image, and three-dimensional image of a whole Raji cell respectively. The scan size was 40 μm. Figure 2.5f–i was the AFM height image, phase image, amplitude image, and three-dimensional image of the cellular local area respectively. The scan size was 4 μm. We can see that the Raji cells trapped by pillars could be imaged by AFM. Cells adhered to the substrate in the vertical direction by poly-L-lysine. Pillars trapped cells in the horizontal direction. This allowed the three-dimensional immobilization of the cells. The imaging results showed the corrugated surface of the living Raji cell. Poly-L-lysine electrostatic adsorption alone can attach mammalian suspended cells onto the substrate, but this adsorption is too weak to acquire AFM images on living cells. We have performed AFM imaging on living Raji cells attached on the substrate by poly-L-lysine, and the results showed that the scanning tip could easily move the cells on the substrate (data not shown). Collectively, the experimental results confirmed that the proposed method was suited to trap living mammalian suspended cells for AFM imaging.

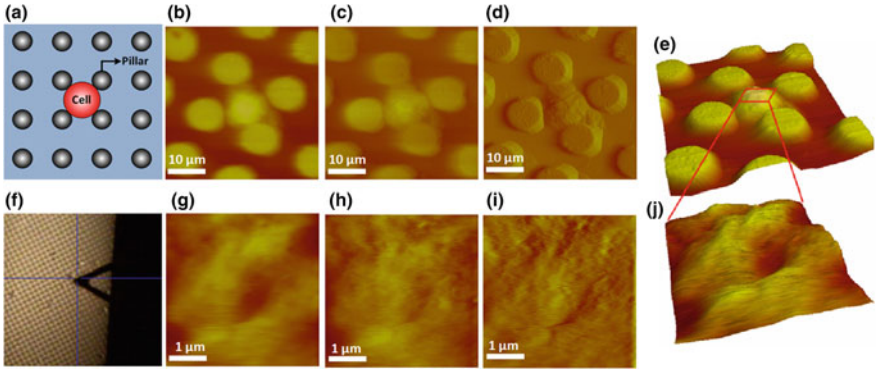

Fig. 2.5 AFM imaging of lymphoma living cells based on the immobilization of pillar mechanical trapping and poly-L-lysine electrostatic adsorption [16]. **a** Principle of mechanical trapping by pillars. (**b**–**e**) AFM images of a whole cell. **b** Height image. **c** Phase image. **d** Amplitude image. **e** Three-dimensional image. **f** Under the guidance of optical image, AFM tip was moved to the trapped cell. (**g**–**j**) AFM images of local area on the cell surface. **g** Height image. **h** Phase image. **i** Amplitude image. **j** Three-dimensional image

2.5 Imaging Living Mammalian Suspended Cells Based on Micro-Well Immobilization

Based on the micropillar chip, polydimethylsiloxane (PDMS) microwell chips were fabricated. Unlike traditional micro-fabrication materials, such as silicon and glass, PDMS is a low-cost material, and PDMS molding processes are simple and rapid [17]. Therefore, we explored fabricating PDMS microwell chips to trap mammalian suspended cells based on the micropillar mold [18]. Liquid PDMS was poured into the pillar mold that was then placed into an 80 °C oven for 2 h. After being separated from the mold, the solid PDMS well chips were acquired. Figure 2.6a is a photo of a PDMS-fabricated well chip and Fig. 2.6e is an optical image of the ordered wells. The height and diameter of the well was 10 and 20 μm respectively. Because PDMS is hydrophobic, the wells should be made hydrophilic before being used for cell immobilization. Hydrophobic wells had rounded drops of PBS, as shown in the AFM images in Fig. 2.6b, c. From the line profile (Fig. 2.6d), we can see that the rounded drop exhibited a parabola shape. If the rounded drop was in the well, cells pushed by the AFM probe could not sink into the well. Several methods can make the PDMS surface hydrophilic, such as plasma cleaning and concanavalin A [19]. We used oxygen plasma to clean the chip for 2 min to make the PDMS surface more hydrophilic, which then allows cells to settle into the wells. AFM images of the chip after being cleaned by oxygen plasma are shown in Fig. 2.6f, g. From the line profile in Fig. 2.6h we can see that the surface wettability of the PDMS ship was enhanced and the rounded drop vanished.

By combining the PDMS microwells and poly-L-lysine electrostatic adsorption, living Raji cells were immobilized for AFM imaging and the results are shown in

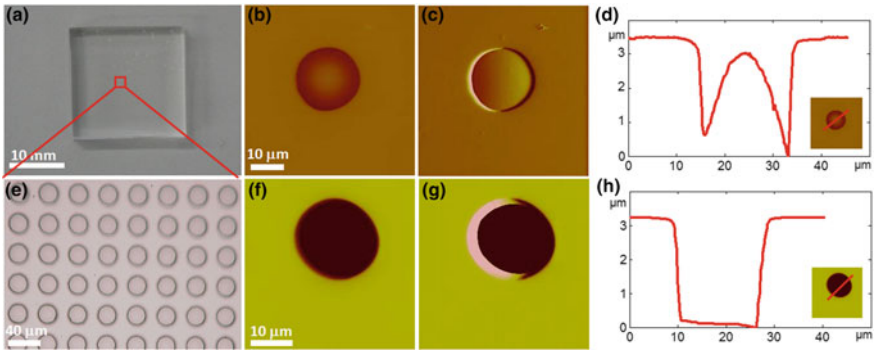

Fig. 2.6 PDMS-fabricated wells and hydrophilic treatment [18]. **a** PDMS well chip. **b–c** AFM images of the PDMS well before plasma cleaning. **b** AFM Height image and corresponding **c** deflection image. **d** Line profile. **e** Optical image of the wells. **f** and **g** were the AFM images of PDMS wells after plasma cleaning. **f** AFM height image and corresponding **g** deflection image. **h** Line profile

Fig. 2.7. Figure 2.7a is the schematic diagram of the immobilization based on microwells. The well can help the cells withstand the lateral scanning force and the poly-L-lysine vertically fixes the cells in the well. AFM images were recorded at tapping mode in PBS. The driving frequency of the cantilever was 9.5 kHz. The scan rate was 0.3 Hz. The scan line was 256 and the sampling point for each scan line was also 256. With the assistance of optical image (Fig. 2.7e), the AFM tip was moved onto a cell trapped in a well (denoted by the circle). Figure 2.7b, d, f shows the AFM height image, three-dimensional rendering of the height image, and phase image of the whole cell, respectively. Figure 2.7c, g, h shows the AFM phase image, amplitude image and the three-dimensional rendering of the height image of a local area on the cell, respectively. In the local area, the cell exhibited a rough and corrugated morphology. If the well was not coated by poly-L-lysine, we found that cells in the wells moved during AFM scanning. Poly-L-lysine thus provides an adhesive force between the cell and the bottom surface of the well. The quality of the AFM images of the whole cell are not as good as those obtained when we used micro-fabricated pillars with electrostatic adsorption to immobilize living Raji cells (Fig. 2.5). This may because that silicon is hydrophilic, while PDMS is hydrophobic. Though oxygen plasma treatment can increase the hydrophilicity of PDMS, thare are still significant differences between silicon and PDMS. Furthermore, silicon is stiff, while PDMS is soft, which may also affect the immobilization. Compared with the images of the whole cell (Fig. 2.7b, d, f), the image quality of the reduced area scans (Fig. 2.7c, g, h) was remarkably improved. This is because that as the scan size decreased, the influence of cell membrane movement decreased ant thus the image quality increased.

The proposed micropillar/microwell immobilization methods can be used to immobilize living mammalian suspended cells for AFM imaging, but notably the acquired AFM images have limited spatial resolution. This is because that the

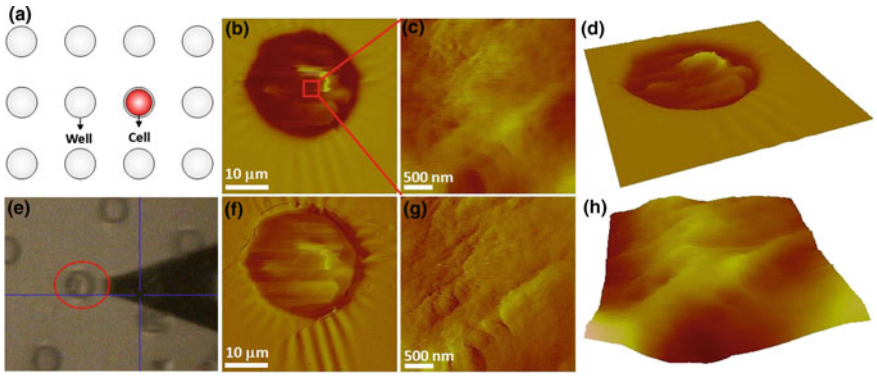

Fig. 2.7 Imaging living Raji cells trapped in PDMS wells in PBS [18]. **a** Principle of well-based trapping. **b** Height images of the whole cell. **c** Phase image of the cellular local area. **d** Three-dimensional image of the whole cell. **e** AFM probe was moved to the trapped cell (denoted by the circle) under the guidance of optical image. **f** Phase image of the whole cell. **g** Amplitude image of cellular local area. **h** Three-dimensional image of the cellular local area

micropillar/microwell immobilization only eliminates the influence of the whole cell on AFM imaging, but cannot eliminate the influence of cytomembrane dynamics on AFM imaging. Dague et al. [19] have used PDMS stamps to trap microbial cells (*Saccharomyces cerevisiae* yeasts and *Aspergillus fumigatus* fungal spores) for AFM imaging. Microbial cells have stiff cell walls, which allows easier acquisition of high quality of AFM images. In contrast, it is challenging to obtain high quality images of softer and larger mammalian suspended cells, since they are easily deformed by the scanning probe [14]. To increase the AFM spatial resolution, methods that can inhibit the dynamics of the cell membrane are required, such as using films which contain small pores of $\sim$100 nm diameter [20]. Cell surface exposed to the pores are relatively rigid and therefore may be imaged. In addition, since the AFM tip can easily deform the soft cell membrane, non-contact AFM imaging techniques, such as scanning ion conductance microscopy (SICM) [14], may potentially improve the spatial resolution of living cell imaging. Novak et al. [21] have used SICM to image the surface living cells with high spatial resolution (about 20 nm). SICM can provide the true topography of soft cells [22], which significantly complements AFM imaging.

2.6 Summary

(1) Biological experiment platform based on AFM nanorobot was established, which was used to image the topography of three different types of living adherent cells.
(2) An immobilization method based on micropillar mechanical trapping and poly-L-lysine electrostatic adsorption was developed, which allowed the

efficient immobilization of mammalian suspended living cells in both horizontal and vertical directions and AFM images of living lymphoma Raji cells were acquired.

(3) Based on the micropillar, PDMS microwell chips were fabricated. By combining microwell mechanical trapping with poly-L-lysine electrostatic adsorption, living Raji cells were immobilized for successful AFM imaging.

References

1. Butt HJ, Wolff EK, Gould SAC et al (1990) Imaging cells with the atomic force microscope. J Struct Biol 105:54–61
2. Chao Y, Zhang T (2011) Optimization of fixation methods for observation of bacterial cell morphology and surface ultrastructures by atomic force microscopy. Appl Microbiol Biotechnol 92:381–392
3. Yang PH, Sun X, Chiu JF et al (2005) Transferrin-mediated gold nanoparticle cellular uptake. Bioconjugate Chem 16:494–496
4. Wu Y, Lu H, Cai J et al (2009) Membrane surface nanostructures and adhesion property of T lymphocytes exploited by AFM. Nanoscale Res Lett 4:942–947
5. Dufrene YF (2004) Using nanotechniques to explore microbial surfaces. Nat Rev Microbiol 2:451–460
6. Matzke R, Jacobson K, Radmacher M (2001) Direct, high-resolution measurement of furrow stiffening during division of adherent cells. Nat Cell Biol 3:607–610
7. Puntheeranurak T, Wildling L, Gruber HJ et al (2006) Ligands on the string: single-molecule AFM studies on the interaction of antibodies and substrates with the Na^+-glucose co-transporter SGLT1 in living cells. J Cell Sci 119:2960–2967
8. Li M, Liu L, Xi N et al (2013) Progress of AFM single-cell and single-molecule morphology imaging. Chin Sci Bull 58:3177–3182
9. Dufrene YF (2008) Atomic force microscopy and chemical force microscopy of microbial cells. Nat Protoc 3:1132–1138
10. Fantner GE, Barbero RJ, Gray DS et al (2010) Kinetics of antimicrobial peptide activity measured on individual bacterial cells using high-speed atomic force microscopy. Nat Nanotechnol 5:280–285
11. Andre G, Kulakauskas S, Chartier MPC et al (2010) Imaging the nanoscale organization of peptidoglycan in living *lactococcus lactis* cells. Nat Commun 1:27
12. Rosenbluth MJ, Lam WA, Fletcher DA (2006) Force microscopy of nonadherent cells: a comparison of leukemia cell deformability. Biophys J 90:2994–3003
13. Ng L, Hung HH, Sprunt A et al (2007) Nanomechanical properties of individual chondrocytes and their developing growth factor-stimulated pericellular matrix. J Biomech 40:1011–1023
14. Muller DJ, Dufrene YF (2011) Force nanoscopy of living cells. Curr Biol 21:R212–R216
15. Deng Z, Lulevich V, Liu F et al (2010) Applications of atomic force microscopy in biophysical chemistry of cells. J Phys Chem B 114:5971–5982
16. Li M, Liu L, Xi N et al (2011) Imaging and measuring the rituximab-induced changes of mechanical properties in B-lymphoma cells using atomic force microscopy. Biochem Biophys Res Commun 404:689–694
17. Jo BH, Lerberghe LMV, Motsegood KM et al (2000) Three-dimensional micro-channel fabrication in polydimethylsiloxane (PDMS) elastomer. J Microelectromech Syst 9:76–81
18. Li M, Liu L, Xi N et al (2013) Atomic force microscopy imaging of live mammalian cells. Sci China Life Sci 56:811–817

19. Dague E, Jauvert E, Laplatine L et al (2011) Assembly of live micro-organisms on microstructured PDMS stamps by convective/capillary deposition for AFM bio-experiments. Nanotechnology 22:395102
20. Ando T (2012) High-speed atomic force microscopy coming of age. Nanotechnology 23:062001
21. Novak P, Li C, Shevchuk AI et al (2009) Nanoscale live-cell imaging using hopping probe ion conductance microscopy. Nat Methods 6:279–281
22. Rheinlaender J, Geisse NA, Proksch R et al (2011) Comparison of scanning ion conductance microscopy with atomic force microscopy for cell imaging. Langmuir 27:697–704

http://www.springer.com/978-981-10-6828-7

Investigations of Cellular and Molecular Biophysical Properties by Atomic Force Microscopy Nanorobotics

Li, M.

2018, XIII, 135 p. 75 illus., Hardcover
ISBN: 978-981-10-6828-7